ENGR7006 – CFD GT3 Coursework

Aerodynamic package design and analysis for a LMGT3 DrivAer fastback smooth floor model

Gr-54

ABSTRACT

As part of the aerodynamics department of a LMGT3 team, we have been commissioned to develop an aerodynamic package for a DrivAer Fastback vehicle. In this report we study the base vehicle model, first validating the mesh that will be used for the different studies, then we perform an analysis on the base vehicle, obtaining pressure, flow speed, drag, lift, front and rear lift forces distribution and ensuring a good quality mesh is maintained during the whole process.

To compare with the improvements made, we will show the development of the components of the front area of the vehicle, when, by making use of the baseline values, we would be able to both discover improvement areas on the vehicle, and later, validate those improvements against the original metrics, then, show the results obtained with the complete package, checking the most efficient set-up of the vehicle by means of an aero map. This map will include an array of configurations in terms of ride height, and will explore the vehicle's behaviour at different yaw angles.

Afterwards, we will share a planning for real world validation of the aero-package by means of wind tunnel testing, where facilities, instruments and measurement procedures will be discussed.

INTRODUCTION

BACKGROUND

In motorsport racing, the LMGT3 series has proved to be one of the leading series providing the manufacturers with a challenge to balance the aerodynamic performance of their vehicles, with strict aerodynamic rules, teams must find the balance between the downforce and the drag produced.

AIMS AND OBJECTIVES

Group Objectives

This project focuses on reviewing, evaluating and validating the aerodynamic performance of the standard DrivAer Fastback vehicle, and improve upon these metrics by developing an aerodynamic package, making use of CAD and CFD software, achieving an improvement over the metrics provided by the base model.

Individual Objectives

The focus of this report is to develop, analyse and validate aerodynamic devices placed in the frontal area of the vehicle, performing an analysis on the device's contribution to the performance metrics of the standard vehicle by itself and with the complete aerodynamic package developed by the team.

METHODOLOGY

GEOMETRY VARIANT INVESTIGATED

The DrivAer Fastback model provided by Technische Universität München was investigated and used for this report, with mirrors and a flat bottom. A full-scale model was used for the analysis of the aero-package, to obtain more accurate pressure coefficient results.

ASSUMPTIONS, LIMITATIONS AND SIMPLIFICATIONS

For the CFD simulations, a steady-state flow was assumed, together with smooth domain walls. For simulations that do not include yaw angle, in order to reduce computational cost, the simulation will be run with a symmetry plane (Soares, R. F., 2015).

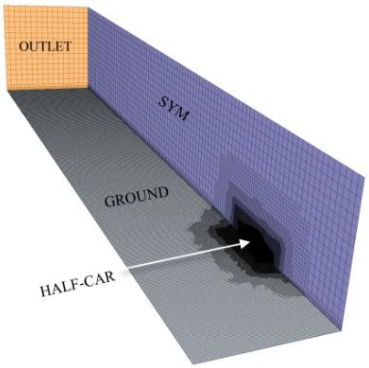

Figure 1. Boundaries of numerical domain over a half-car model

Closed wheels, flat vehicle underbody and no cooling ducts were used in the model, rotating wheels were excluded from the frontal area aero-package study to reduce computational cost.

NUMERICAL APPROACHES IMPLEMENTED

Meshing and mesh optimization

The steady-state 3D RANS equations model was used, as it has been proven both accurate and reliability for steady state flow, together with a K- ω turbulence model, as this combination is both computationally inexpensive, easy to configure and reliable for steady-state flow, up to 25 degrees of yaw.

First, we selected a coupled flow, as it allows for a faster convergence, better representation of on-surface metrics and better stability on high-speed flows, then, the K-ω turbulence model is chosen, as it stands above the K-$\sum$ turbulence for this test, as this model allows for a better representation of separation produced on the vehicle's body (Versteeg, H. K., 2007; Ashton, N., 2015).

METHODOLOGY FLOW CHART

To develop the aero-package, a development process methodology was put in place, to allow a more organized and fail-proof workflow.

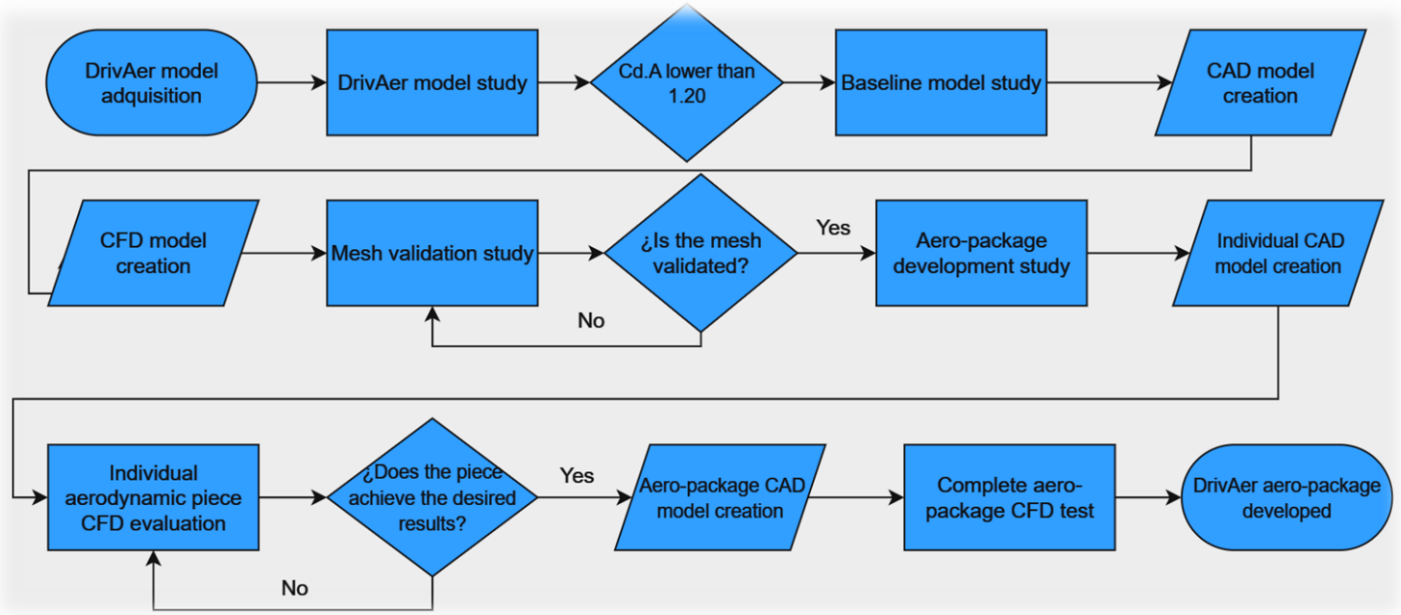

Figure 2. Aero-package development methodology flow chart

RESULTS AND DISCUSSION

BASELINE DRIVAER

For the baseline DrivAer validation, the TLU Fastback model at full-scale was used.

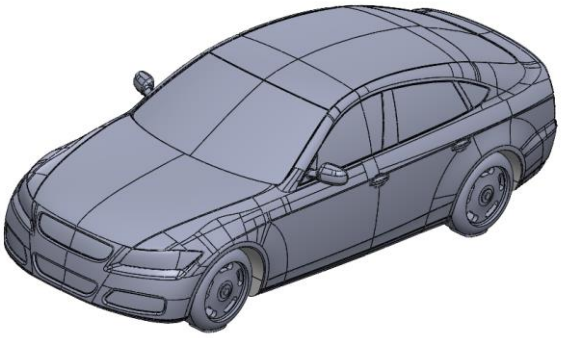

Figure 3. TLU DrivAer Fastback model

To validate the meshes to be used for the analysis of the aero-package behaviour, the results obtained were compared with the results of Qin, P., Ricci, A., Blocken, B. (2024), since for their analysis, the same configurations that we were going to use were used, making use of the RANS model, coupled flow and K-omega turbulence.

The results achieved in their study were validated with a wind-tunnel study of a 1:4 DrivAer Fastback model with smooth underbody, increasing the credibility of the results achieved. It also compares its results with other well-known DrivAer validation CFD papers, such as Heft et al., 2012; Wieser et al., 2014; Soares et al., 2018 and Varney et al., 2020, among others.

The dimensions of the computational domain used for the simulations are based on the dimensions of Qin, P., although our simulations considered a symmetry plane on the vehicle to ease computational costs.

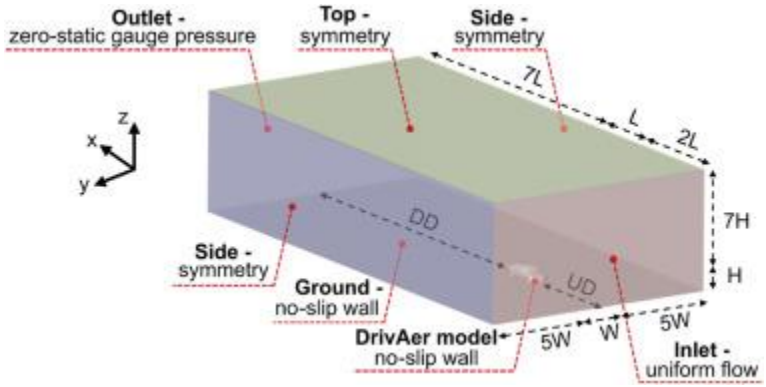

Figure 4. Computational domain measurements

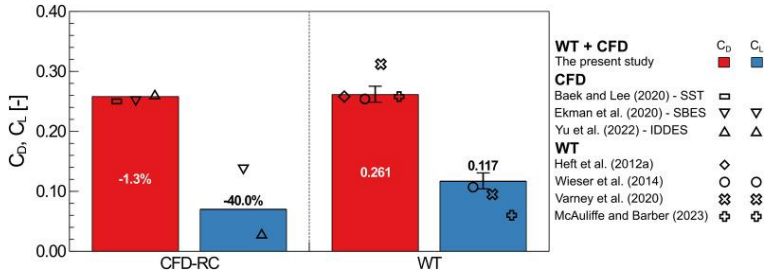

Figure 5. Comparison between Qin, P.'s CFD reference case and WT test

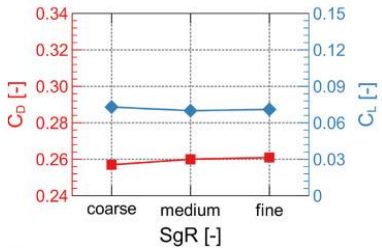

Figure 6. Qin, P.'s Impact of surface grid resolution on Cd and Cl

Achieved results show a Cd value of ~0.288 and a Cl value of ~0.072.

For our mesh convergence study, 7 different meshes were tried, achieving the following results:

Table 1. Mesh convergence study results

	Mesh 1	Mesh 2	Mesh 3	Mesh 4	Mesh 5	Mesh 6	Mesh 7
Speed	50m/s	50m/s	50m/s	50m/s	50m/s	50m/s	50m/s
Cd	0.276391	0.297700	0.283660	0.298977	0.288677	0.289236	0.289784
Cl	0.065077	0.091562	0.076490	0.085465	0.091139	0.089614	0.09037665
Cells	257,092	257,092	734,145	978,676	1,905,556	2,764,325	6,445,326
Rotating wheels + moving floor	No	Yes	Yes	Yes	Yes	Yes	Yes

Table 2. Mesh convergence study graphical evolution

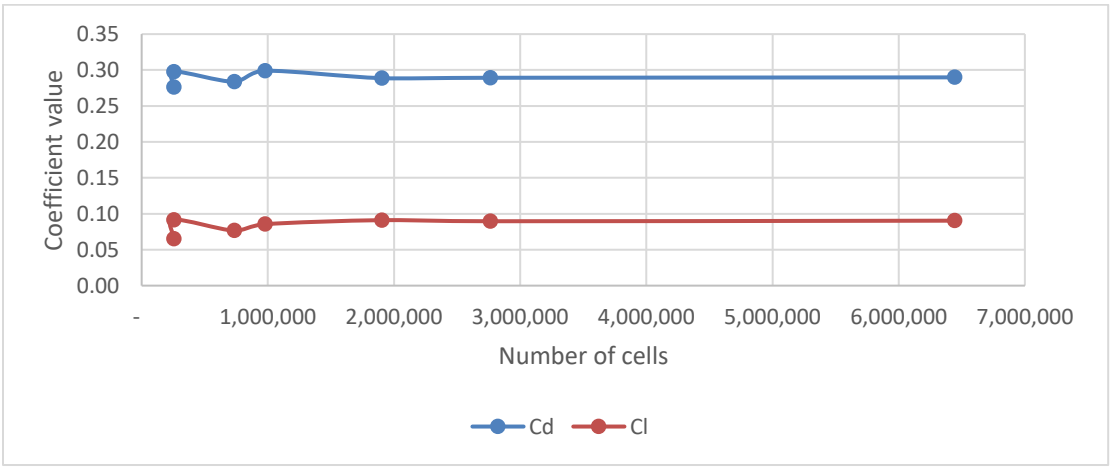

Comparing our results with those obtained in Qin, P.'s research, we can conclude that the optimum mesh is 1,905,556 cells, achieving an insignificant difference in values from there.

This mesh will be used from now on for the rest of the studies carried out in this report, the mesh values are attached in the appendix, along with the continua physics settings, in tables 6 and 7, respectively.

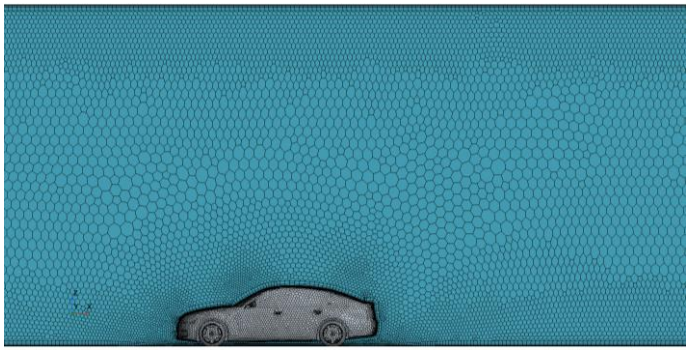

Figure 7. Lateral view of optimized mesh

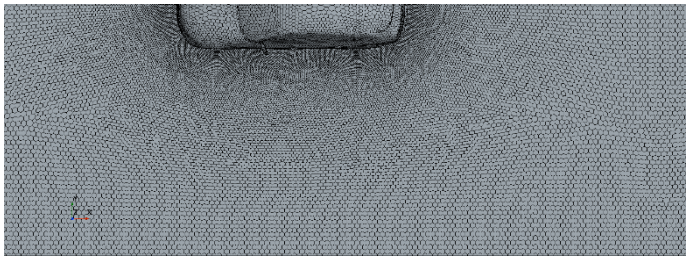

Figure 8. Top view of optimized mesh

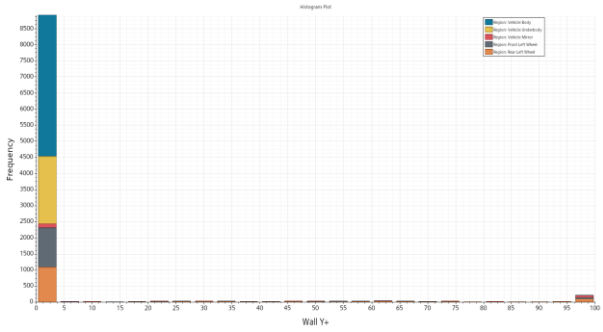

Figure 9. Wall Y+ values for the optimized mesh

Results for the baseline model behaviour can be seen below.

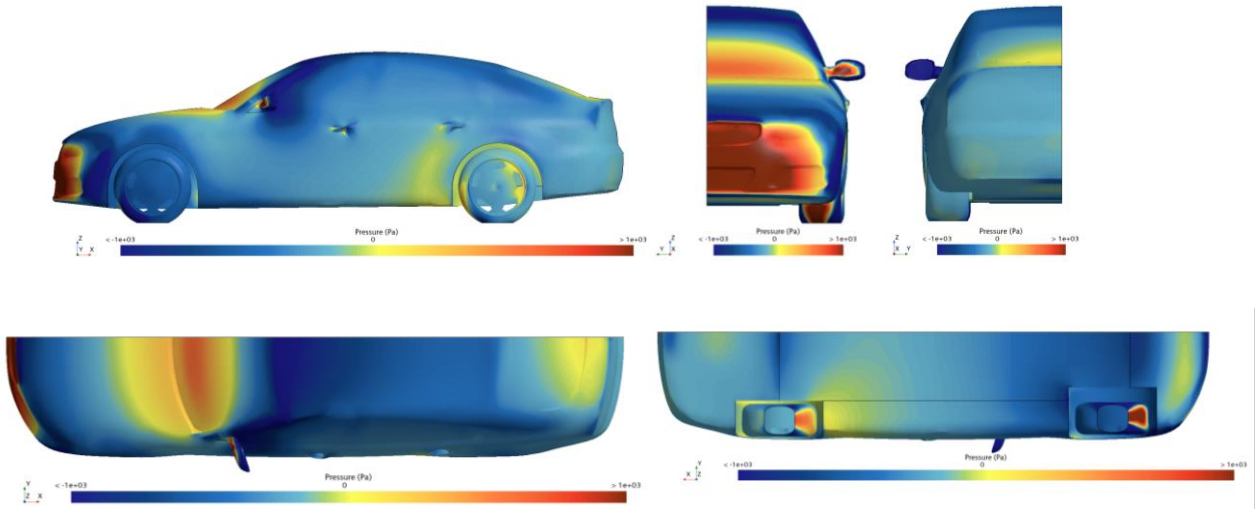

Figure 10. Pressure distribution along the baseline model surface

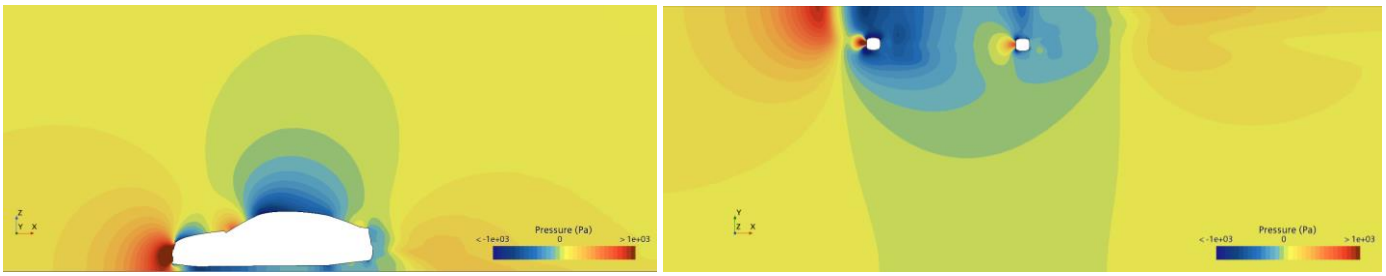

Figure 11. Pressure distribution around the baseline model

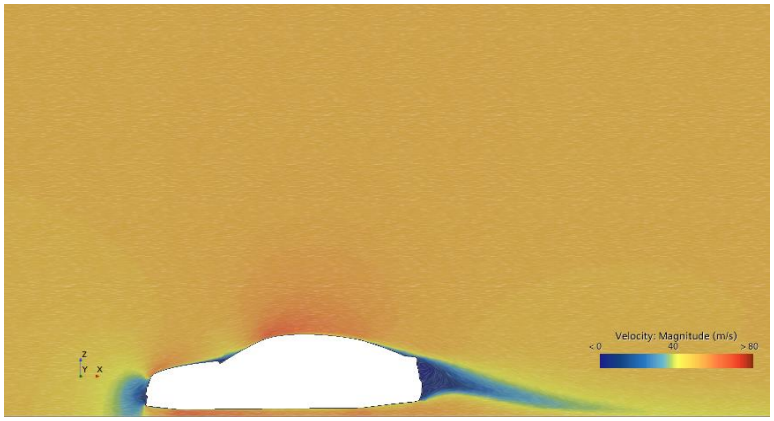

Figure 12. Fluid velocity around baseline model

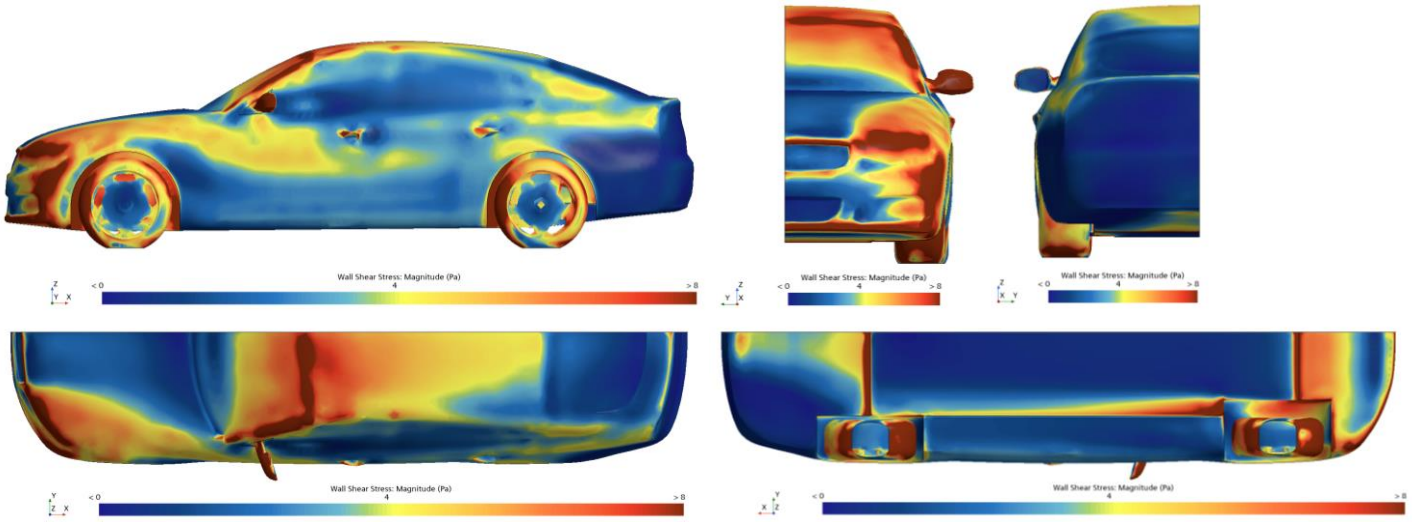

Figure 13. Wall shear stress along the baseline model surface

From these charts we can see that the baseline model has a high stagnation point at the front bumper and, although the flow remains attached to the vehicle along the roof, sides and underbody, we can observe a large wake at the rear of the vehicle, which contributes greatly to the overall drag of the vehicle and results in flow separation, which can be confirmed by the data shown in the velocity chart.

By analysing the stagnation at the front of the vehicle, using the pressure plot, we can confirm the existence of an area of high pressure, which can indicate the ideal position to place a splitter to maximise the downforce generated.

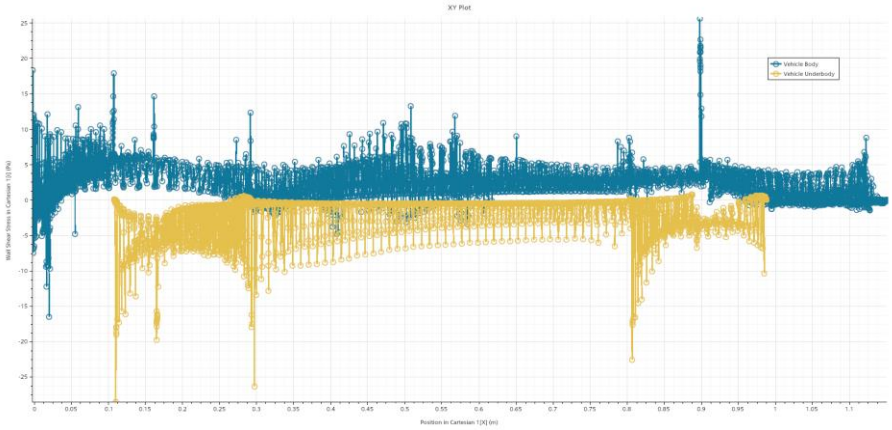

Figure 14. Wall shear stress for baseline model

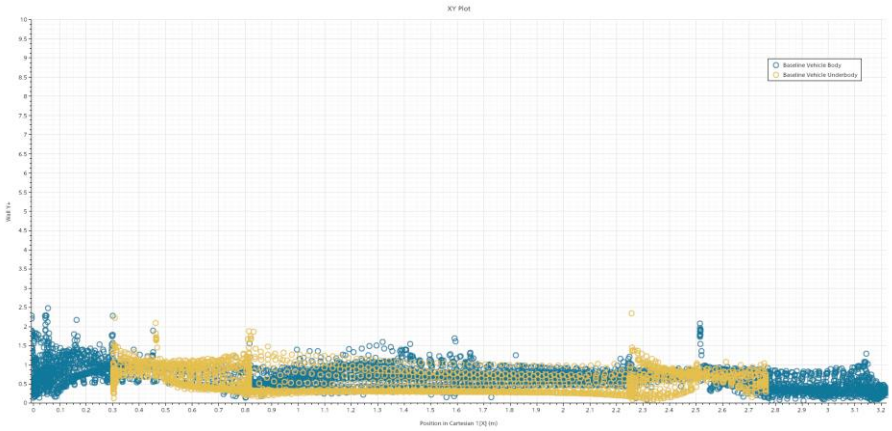

Figure 15. Wall Y+ for baseline model

From these plots, we can observe that there is some separation occurring on the underbody of the vehicle, while the mesh quality is maintained at a good level.

AERO PACKAGE DRIVAER

Frontal area aero-package

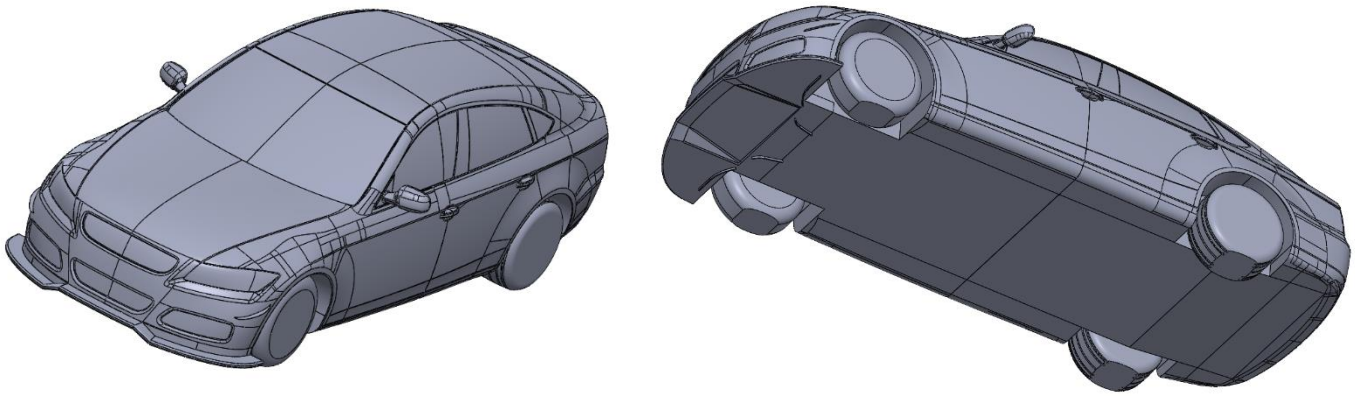

Figure 16. DrivAer Fastback model with Splitter add-on

To start the development of the frontal area components, research was conducted, in order to make educated decisions on the design.

A study conducted by Bhattcharjee, S., found that, for a NASCAR 2019 vehicle of similar dimensions to the DrivAer model, an increase of splitter overhang length, leads to an increase in downforce, thus indicating us that the optimal splitter overhang would be the maximum allowed by regulations.

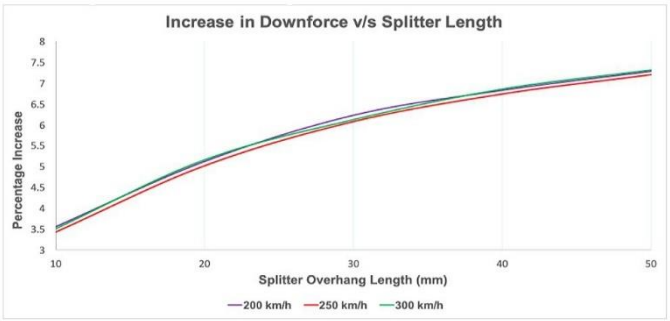

Figure 17. Percentage increase in downforce with respect to splitter overhang length

On another study, conducted by R. F. Soares, the effects of canards on an enclosed-wheel racing car are discussed. It is then said that, if in need of front downforce, the addition of canards would make an improvement.

Additionally, Nakata, A. investigated about the impact on overall drag of deflectors positioned before the front wheels.

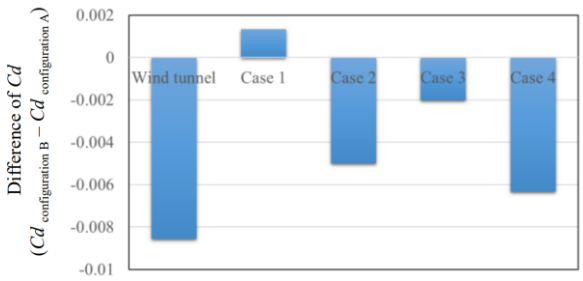

Figure 18. Variations in Cd values when changing the deflector configuration

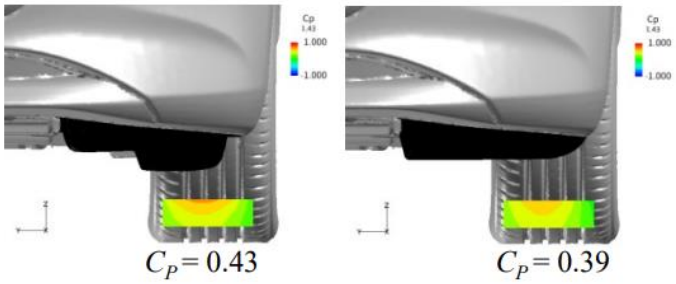

Figure 19. Pressure distributions in front of the tyre

Acquired this knowledge, and implementing Venturi effect geometry to move the flow to the centreline of the vehicle, the splitter presented in figure 14 was designed, design parameters to confirm the legality of the designed part are available as table X in the annex. Closed front wheels and extended and closed rear wheels were also implemented to the model.

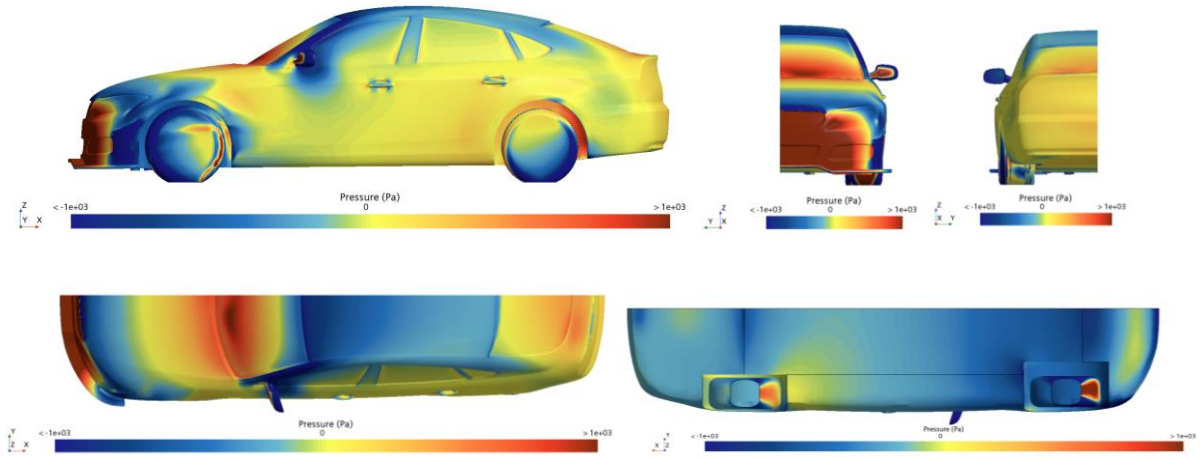

Figure 20. Pressure distribution along the splitter model surface

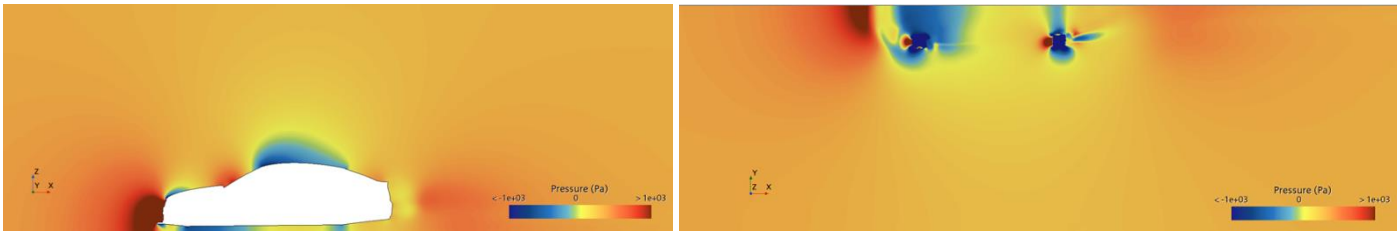

Figure 21. Pressure distribution around the splitter model

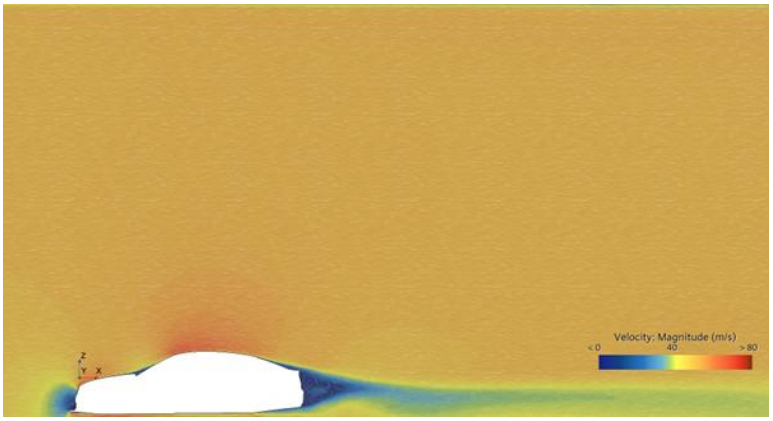

Figure 22. Fluid velocity around splitter model

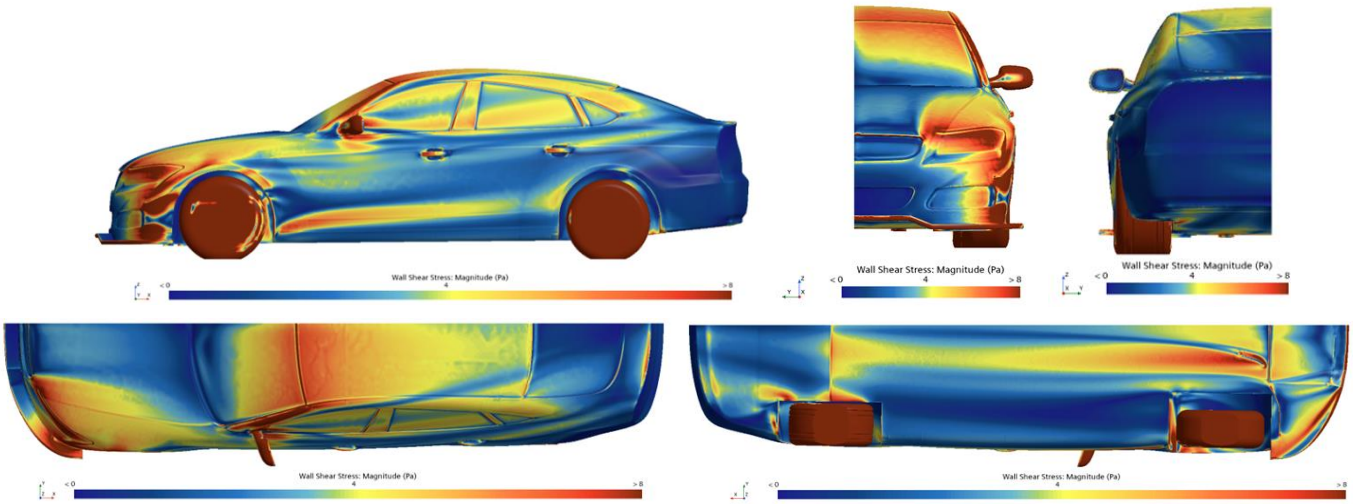

Figure 23. Wall shear stress along the splitter model surface

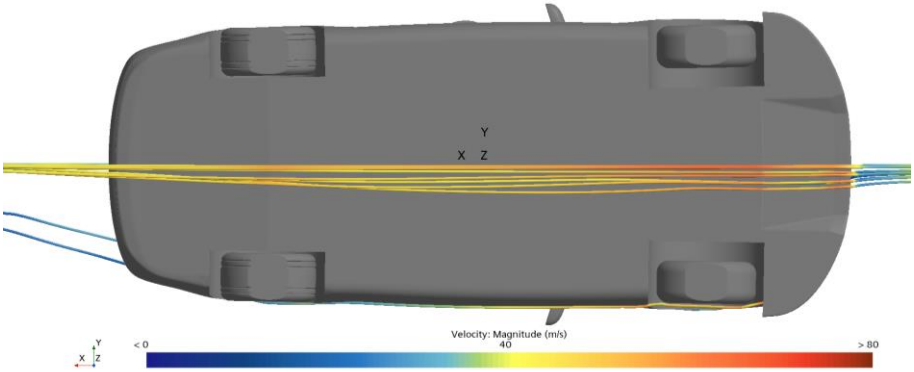

Figure 24. Splitter model underbody velocity streamlines

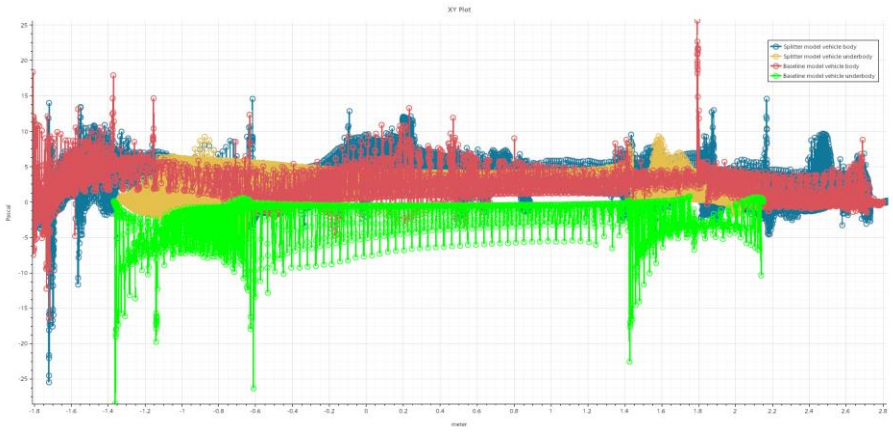

Figure 25 Wall shear stress comparison with baseline

Figure 26. Wall Y+ comparison with baseline

Overall, we can see an improvement on the underbody wall shear stress, meaning less separation is occurring at the vehicle's floor, as the value deviates less than the baseline counterpart, while the body shear stress and both Wall Y+ are maintained roughly at the same value, indicating an overall improvement over the baseline.

	Baseline model	Splitter model
Drag Coefficient	0.288677	0.32843
Lift Coefficient	0.091139	-0.1077338
Front Lift Force	-32.38501	-626.65
Rear Lift Force	38.42735	-16.90

Although drag sees an increment, it is the change on lift force generated we are interested in, as, contrary to the baseline, the splitter model is generating downforce instead of lift, improving the vehicle handling.

Full vehicle aero-package

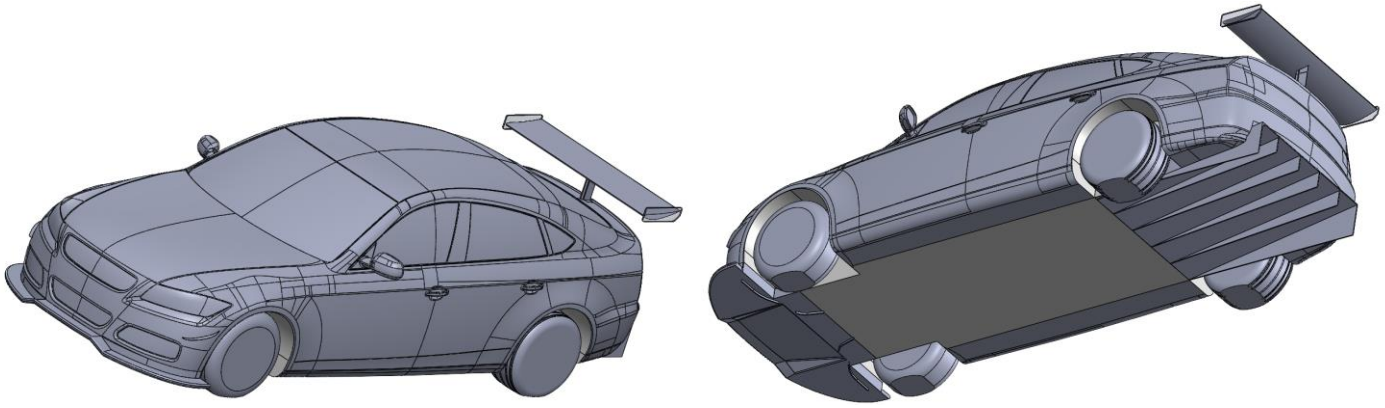

Figure 27. DrivAer Fastback model with aero-package add-on

Once the complete aero-package was assembled, we run an aerodynamic map study, where we varied the front and rear ride heights, to find the best configuration possible to run our vehicle. The results were the following:

Table 3. Aerodynamic map performed on complete aerodynamic package

		Rear ride height (m)				
	Cd	0.1	0.09	0.08	0.07	0.06
Front ride height (m)	0.1	0.388	0.401	0.429	0.422	0.414
	0.09	0.394	0.368	0.369	0.373	0.377
	0.08	0.404	0.391	0.379	0.371	0.387
	0.07	0.401	0.370	0.338	0.375	0.375
	0.06	0.411	0.361	0.348	0.341	0.361

		Rear ride height (m)				
	Cl	0.1	0.09	0.08	0.07	0.06
Front ride height (m)	0.1	-0.452	-0.439	-0.447	-0.455	-0.352
	0.09	-0.418	-0.486	-0.371	-0.347	-0.322
	0.08	-0.408	-0.385	-0.361	-0.368	-0.312
	0.07	-0.456	-0.407	-0.358	-0.326	-0.338
	0.06	-0.446	-0.336	-0.348	-0.356	-0.289

		Rear ride height (m)				
	Cl/Cd	0.1	0.09	0.08	0.07	0.06
Front ride height (m)	0.1	-1.164	-1.096	-1.042	-1.078	-0.851
	0.09	-1.063	-1.320	-1.006	-0.930	-0.856
	0.08	-1.012	-0.983	-0.953	-0.991	-0.808
	0.07	-1.137	-1.101	-1.059	-0.871	-0.901
	0.06	-1.085	-0.930	-1.000	-1.043	-0.801

		Rear ride height (m)				
	Aerodynamic Balance (% of Front effect)	0.1	0.09	0.08	0.07	0.06
Front ride height (m)	0.1	0.840	0.853	0.700	0.693	0.588
	0.09	0.852	0.949	0.744	0.664	0.583
	0.08	0.862	0.808	0.754	0.747	0.593
	0.07	0.759	0.785	0.763	0.792	0.816
	0.06	0.769	0.762	0.772	0.668	0.882

From the results, we can see that the vehicle is producing much more downforce at the front than at the rear, ideal aerodynamic balance should be at 50% distribution for both the front and the rear, however, the most repeated value for our package is 70% bias to the front of the vehicle.

This result tells us that the best configuration for our vehicle would be at 0.9m ride height at both the front and rear axles, as that's where the Cl/Cd achieves the highest ratio. The results from that configuration are the following:

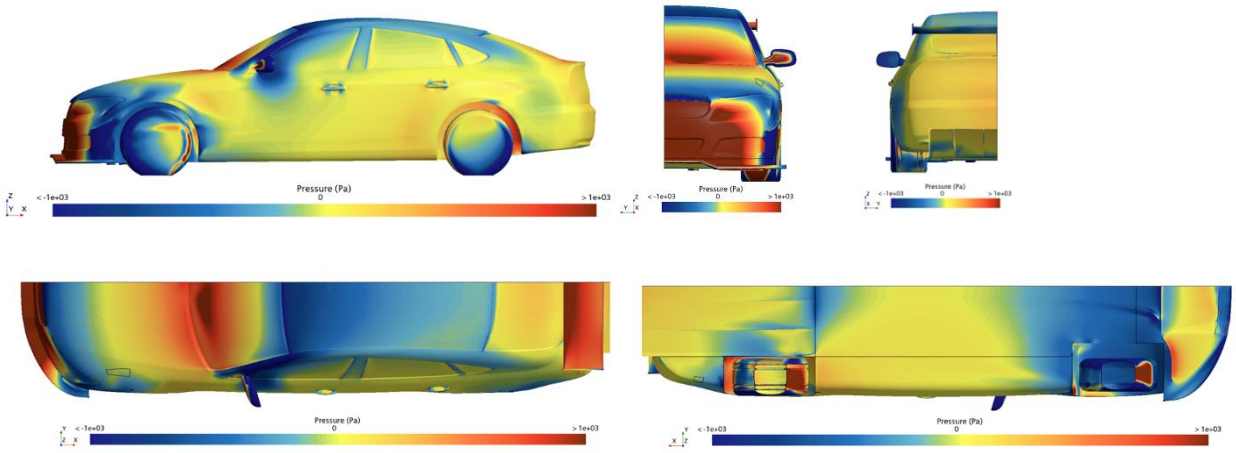

Figure 28. Pressure distribution along the aero-package model surface

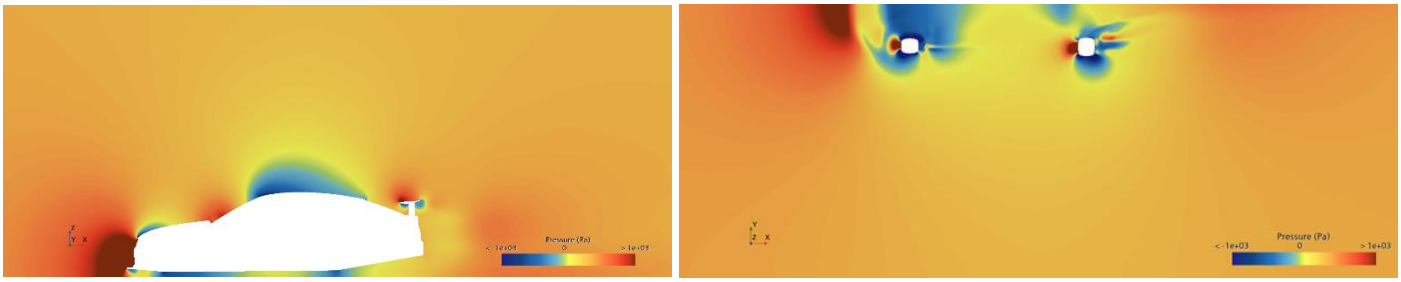

Figure 29. Pressure distribution around the aero-package model

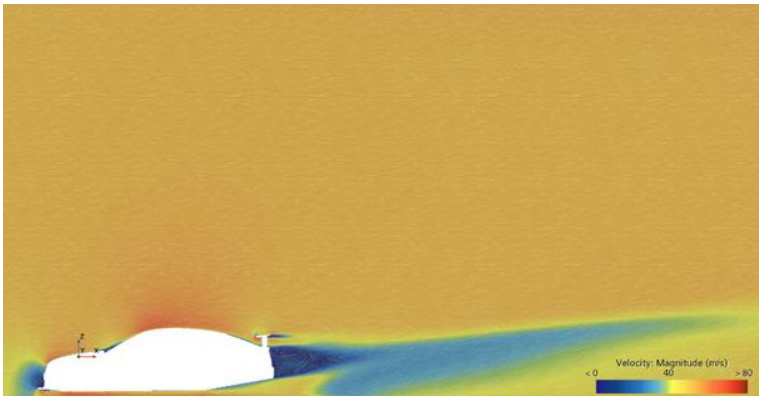

Figure 30. Fluid velocity around optimal aero-package model

Looking into the velocity plot available on figure 30, we can see that the floor accelerates the fluid, reducing the wake present on the vehicle, compared against the plot available in figure 31, where the worst configuration is shown, we see that the separation behind the vehicle is worse than the baseline, creating a bigger wake and an unstable vehicle.

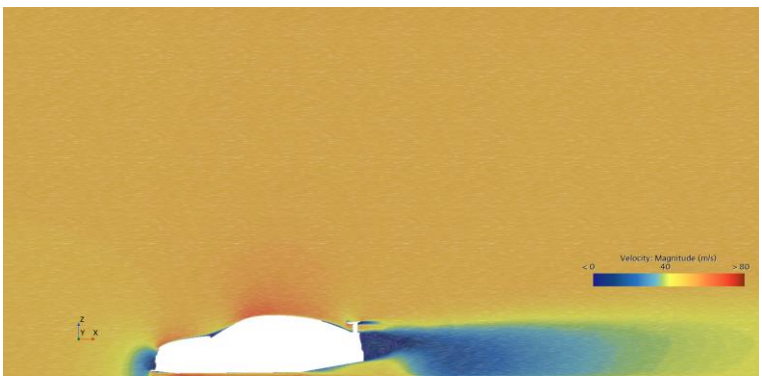

Figure 31. Fluid velocity around worst aero-package model configuration

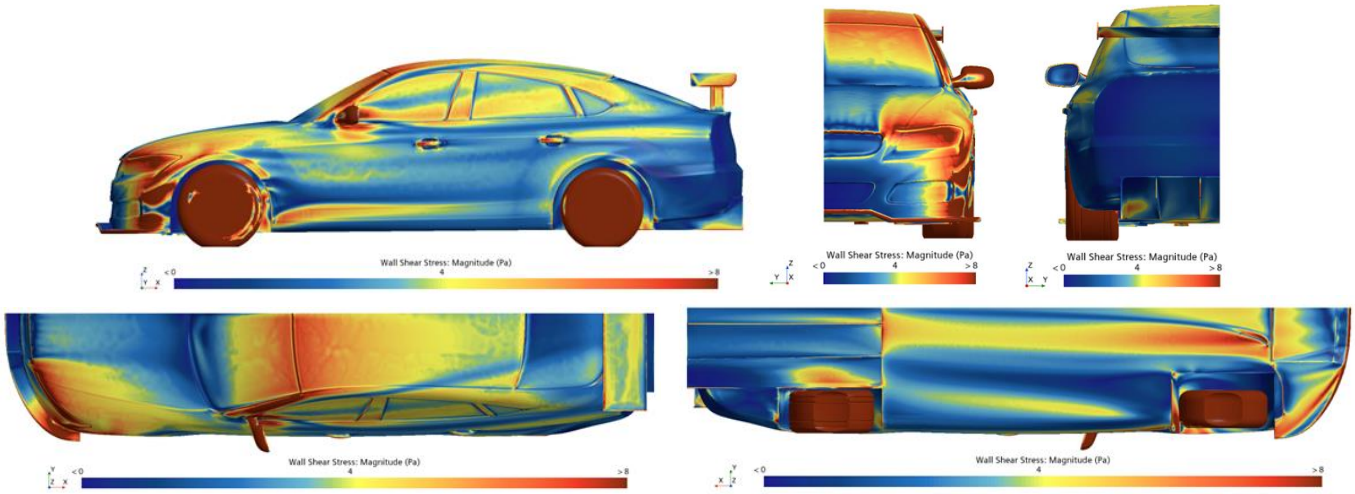

Figure 32. Wall shear stress along the aero-package model surface

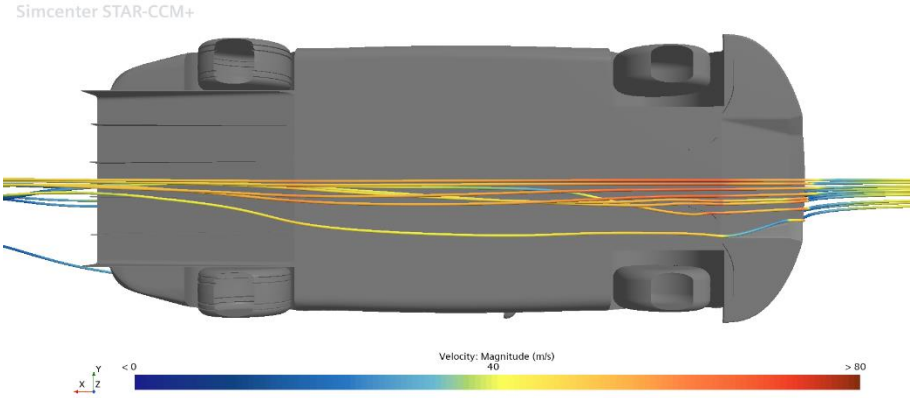

Figure 33. Aero-package model underbody velocity streamlines

Looking into the streamlines, we can see how the air gets accelerated as it enters the underbody on the splitter while its being pushed to the centreline of the vehicle.

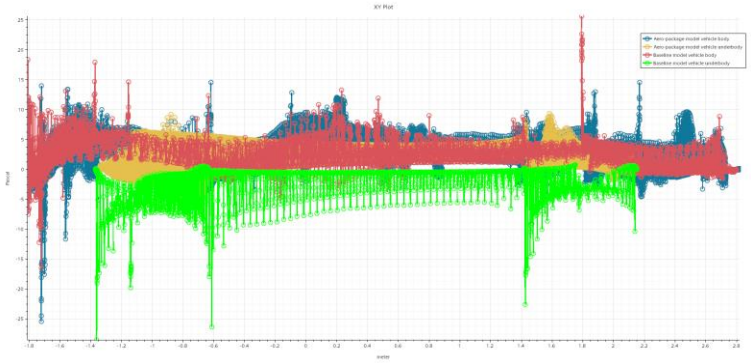

Figure 34. Wall shear stress aero-package comparison with baseline

The vehicle achieves less separation with the added aero-package, compared to the baseline.

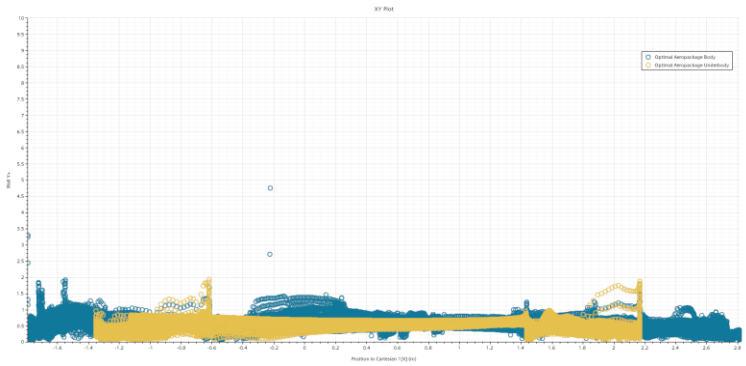

Figure 35. Aero-package wall Y+ values

Table 4. Forces comparison between models

	Baseline model	Splitter model	Optimal aero-package	Worst aero-package
Drag Coefficient	0.288677	0.32843	0.368	0.361
Lift Coefficient	0.091139	-0.1077338	-0.4485842	-0.30752
Front Lift Force (N)	-32.38501	-626.65	-573.5142	-489.036
Rear Lift Force (N)	38.42735	-16.90	-143.5936	-2.51625
Cl/Cd	0.315713	-0.328027	-1.218979	-0.85186

On this table we can observe the effect the aero-package has on the vehicle's performance, implementing an upgrade, to the vehicle's handling even in its worse state.

Additionally, according to the rule set, the Cd.A required to achieve a good performing aero-package is 1.02. For this aero-package, frontal area has a value of 2.16m^2, achieving a Cd.A for the optimal aero-package of 0.79488, far below the maximum admissible value, while achieving a Cl/Cd of -1.218979.

Full aero-package yaw configurations

After creating the aerodynamic map, simulations with the full aero-package were done to characterize the behaviour at different yaw angles. The yaw angles chosen where 5, 10 and 15 degrees, based on the technical paper written by Wieser, D., et al., 2014.

Wieser proposes values for yaw angles of 5 and 10 degrees, first, let's validate our result data for pressure coefficient, to confirm the validity of the data and confirming the values achieved for the 15 degrees of yaw angle. The yaw angle used by Wieser is inverted to the one used in our tests. At the left, we will see the values achieved by Wieser, at the right, we will see our values.

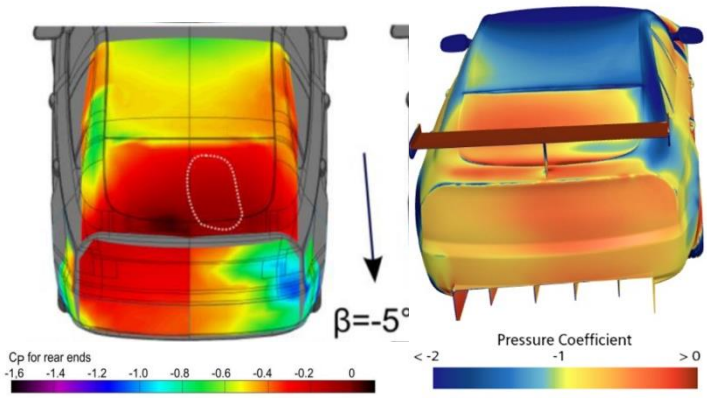

Figure 36. Validation for 5 degrees of yaw angle

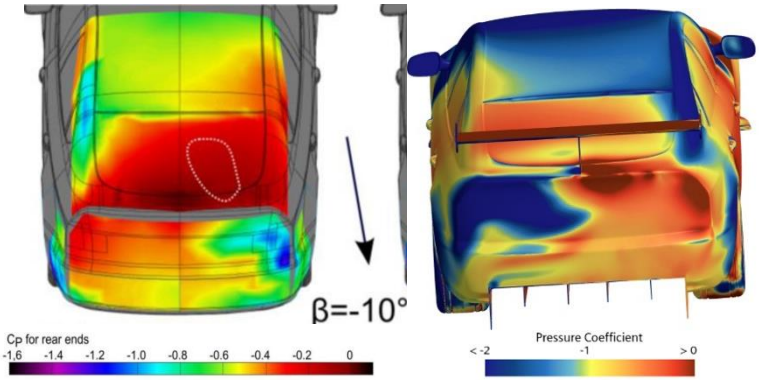

Figure 37. Validation for 10 degrees of yaw angle

Although they are inverted, we can confirm a similar amount of pressure on the vehicles, achieving a low pressure/ high speed zone at the corner opposite to the yaw, where the vortex will be generated.
Now that we have confirmed the validity of our data, we can represent the full data for the 3 yaw angles selected.

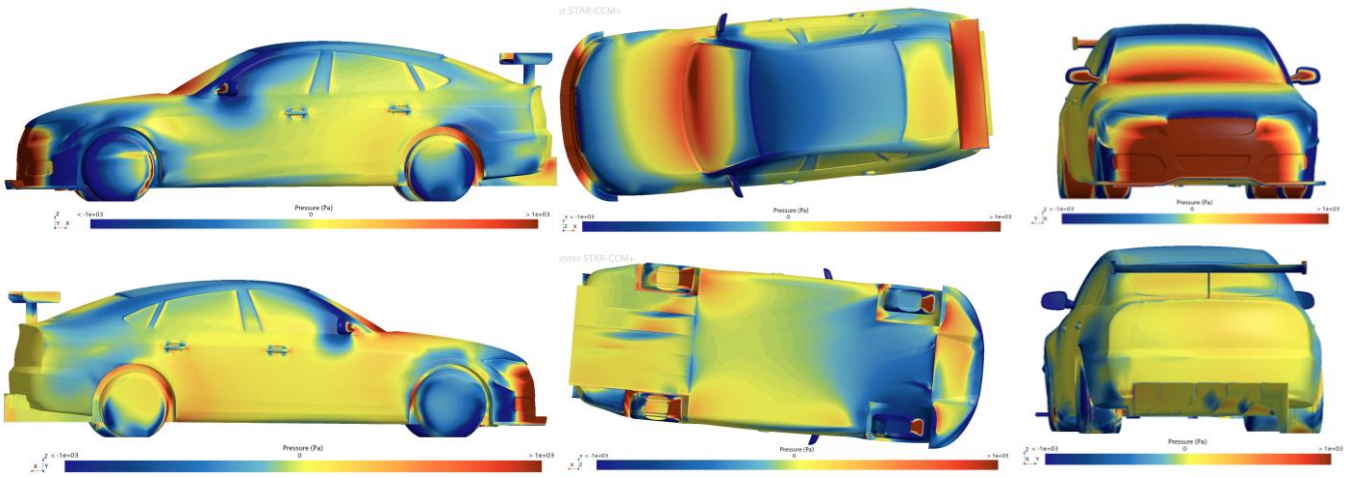

Figure 38. 5 degrees of yaw – On surface pressure

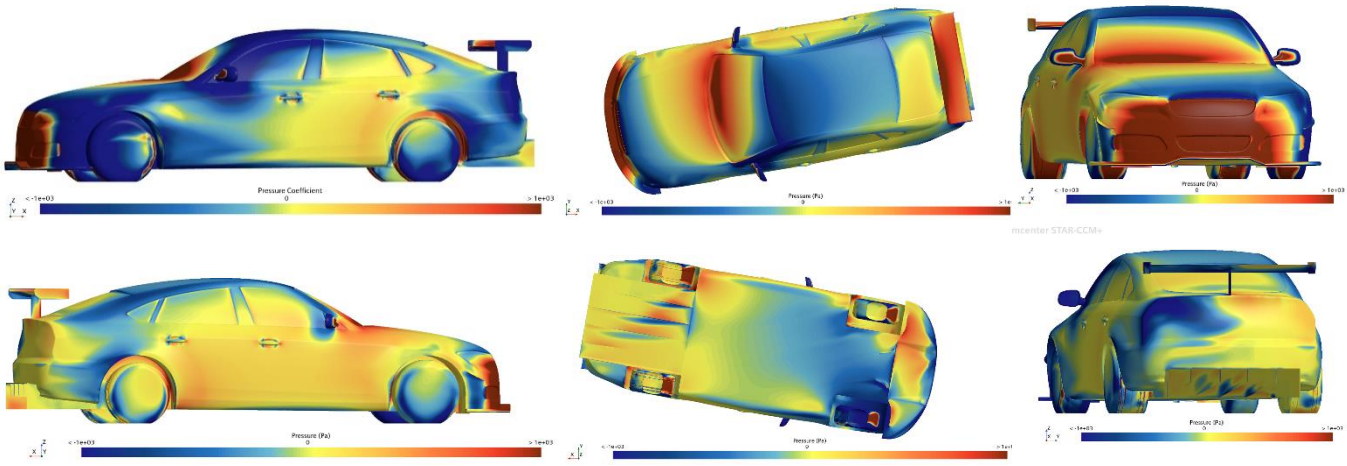

Figure 39. 10 degrees of yaw – On surface pressure

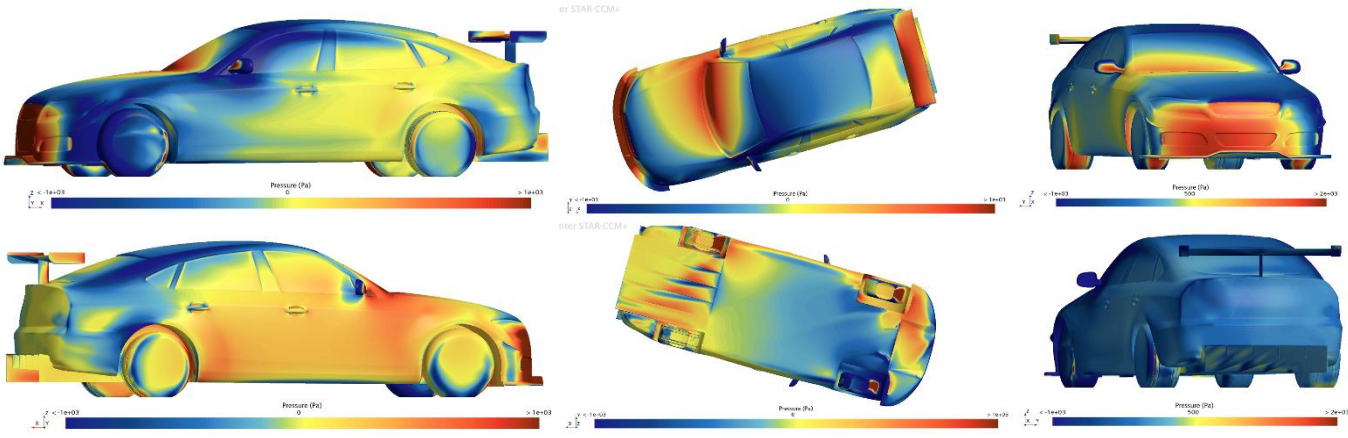

Figure 40. 15 degrees of yaw – on surface pressure

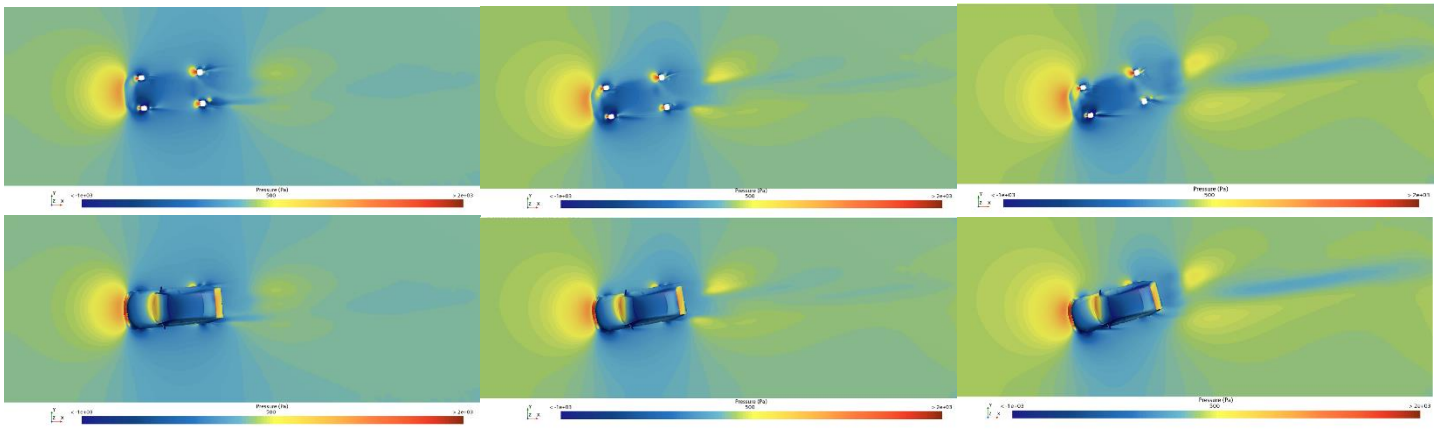

Figure 41. 5 deg. of yaw - Domain pressure *Figure 42*. 10 deg. of yaw - Domain pressure *Figure 43*. 15 deg. of yaw - Domain pressure

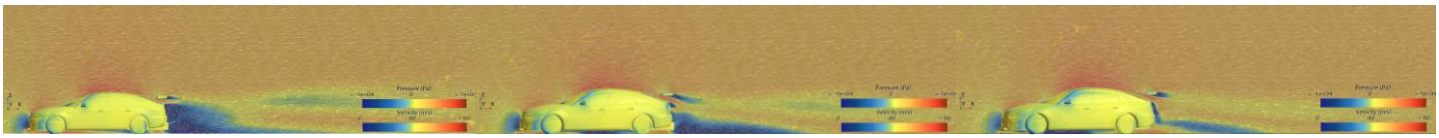

Figure 44. 5 deg. Domain vel. & pressure *Figure 45*. 10 deg. domain vel. & pressure *Figure 46*. 15 deg. domain vel. & pressure

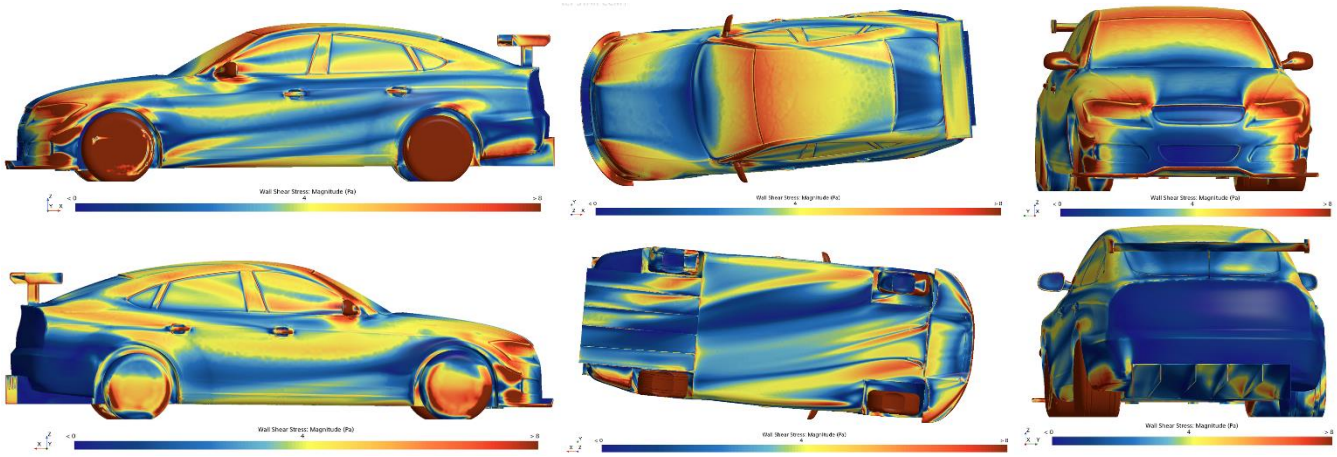

Figure 47. 5 degrees of yaw – Wall shear stress

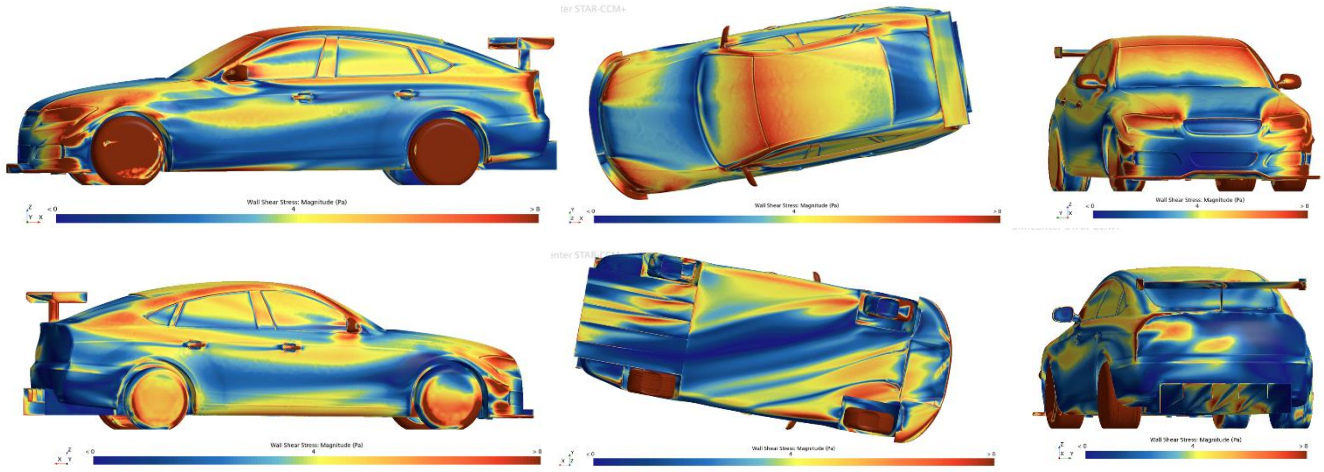

Figure 48. 10 degrees of yaw – Wall shear stress

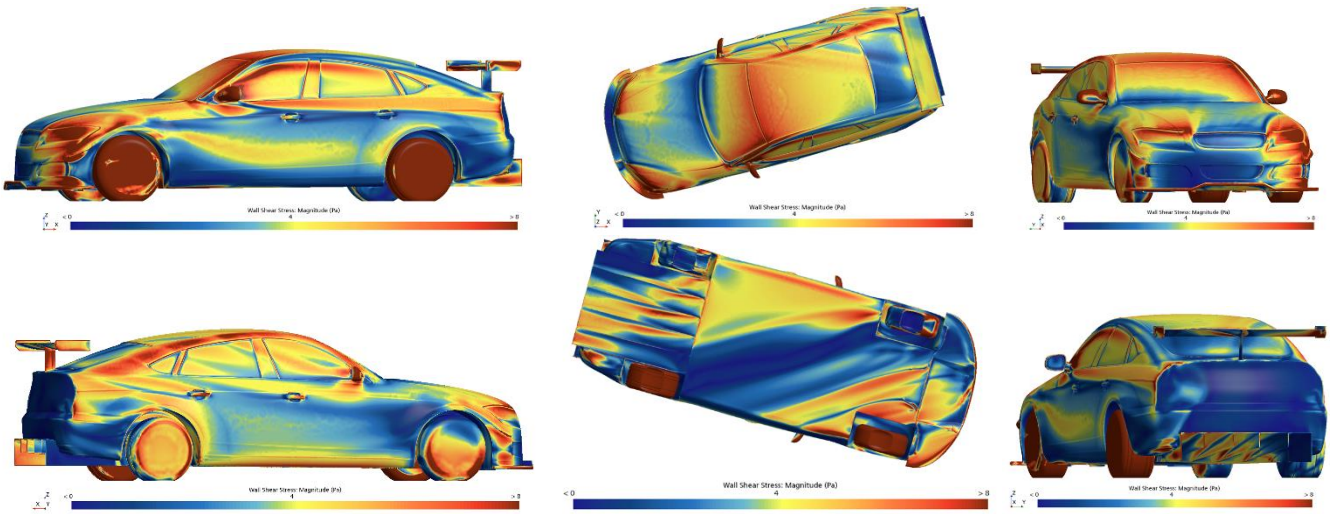

Figure 49. 15 degrees of yaw – Wall shear stress

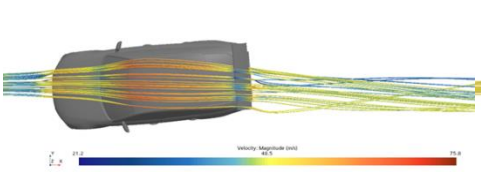

Figure 50. 5 deg. Velocity streamlines

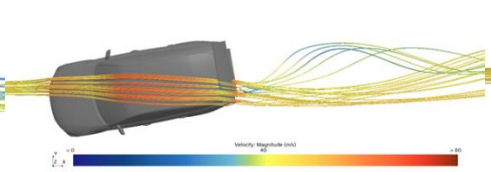

Figure 51. 10 deg. Velocity streamlines

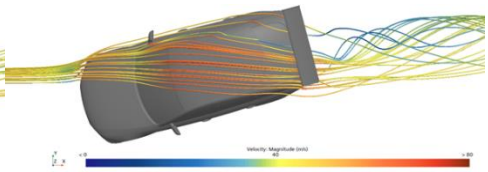

Figure 52. 15 deg. Velocity streamlines

From these graphs we can observe the effects of crosswinds on vehicle behaviour, even at 5 degrees where the flow seems mostly still symmetrical, where a little vortex can be seen start forming with the streamlines. At 10 degrees, the flow starts to be noticeable asymmetrical, being visible the higher pressure of the leading side of the vehicle compared to the trailing side, as the flow detaches from the surface. At 15 degrees of yaw, the flow becomes really skewed, almost skyping the diffuser completely as the flow detaches. Vortices generated at 15 degrees are clearly visible, introducing a really big and unstable wake at the rear and trailing edge of the vehicle.

The functionality of the strakes applied to the underside of the vehicle are really visible here, as the flow is redirected by them, so that it does not reach the tyre, but is redirected towards the diffuser, helping to reduce the unstable handling characteristics generated by yaw.

	0 degrees of yaw	5 degrees of yaw	10 degrees of yaw	15 degrees of yaw
Drag Coefficient	0.368	0.42742	0.5553525	0.6217204
Lift Coefficient	-0.4485842	-0.2565175	-0.2058192	-0.08914375
Front Lift Force (N)	-573.5142	-916.2681	-963.9149	-840.04782
Rear Lift Force (N)	-143.5936	96.12907	305.86857	555.03698
Cl/Cd	-1.218979	-0.6001532	-0.370661	-0.1433824

We can observe that, as yaw angle increases, the overall downforce decreases, as flow separation increases.

EXPERIMENTAL VALIDATION METHODOLOGY

WIND TUNNEL/TRACK SETUP

As we have done our CFD validation and testing of our aero-package for a full-scale model at 50m/s with a moving floor, to validate the results achieved, it would be appropriate to replicate the same dimensions and conditions. For this reason, the RRWT facility (Nagle, P., 2023) is selected as the appropriate wind tunnel for the validations.

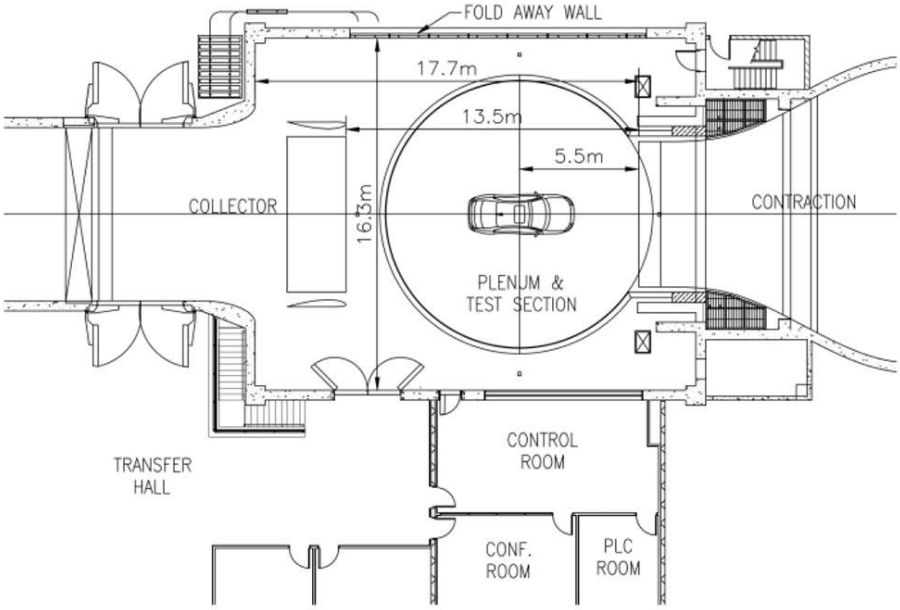

Figure 53. Birds-eye view of the RRWT facility

This wind tunnel is a low speed, closed-loop tunnel, with a working section of 17.7 m in length, a 5.5 m space between the vehicle and the nozzle outlet and a width of 16.3 m, dimensions that match the domain used for our CFD simulations.

The wind tunnel also features two different nozzles, capable of wind speeds of up to 322 km/h, which allowed us to reach our test speed of 180 km/h, with capabilities of testing the top speed of 300km/h required by the LMGT3 regulations.

The tunnel features a 5-belt MGP, with capabilities up to 250 km/h, a 6-component force balance and a turntable capable of achieving ±30 degrees yaw angle also allows us to further validate the results achieved for drag, lift, pitch and yaw of our CFD simulations.

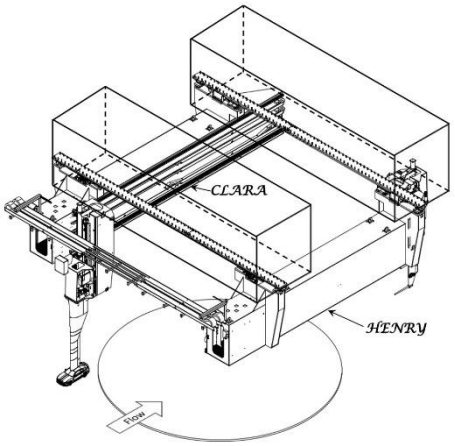

Figure 54. Dual flow traverses

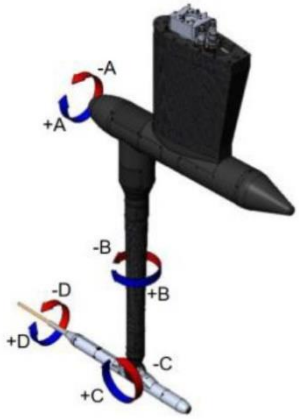

Figure 55. 4-Axis Probe Manipulator showing axes of rotation

The tunnel also features a dual flow traverse system, which is of extremely importance for motorsport testing, such as out testing with the LMGT3 DrivAer model, where, if using up to a 60% scale model, allows us to study tandem vehicle situations.

This system records data with a 4-axis probe manipulator, and optical measurements, with the possibility to add PIV lasers and cameras.

EQUIPMENT AND MEASUREMENTS

For data recollection purposes, the experiment will make use of the force balance system available in the wind tunnel, to obtain drag, lift and side forces, together with yaw, pitching and rolling moments.

Pressure taps along the vehicle should also be used, these will be chosen based on the information given by Barlow J. B, Rae, W. H. and Pope, A. in the chapter 4 of the book “Low-speed wind tunnel testing”.

- Pressure measurements: To allow for pressure measurements, pressure taps, and PSP could be used, however, PSP will not be used, due to the expensive nature of the method.

- Flow measurements: Pitot tubes are reliable up to 8 degrees of flow inclination, after that, Kiel tubes can be used reliably until 30 degrees of inclination. For our test, we will rely on 2 Pitot tubes, one placed in free stream conditions, and another placed in front of the splitter, to capture incoming flow conditions.

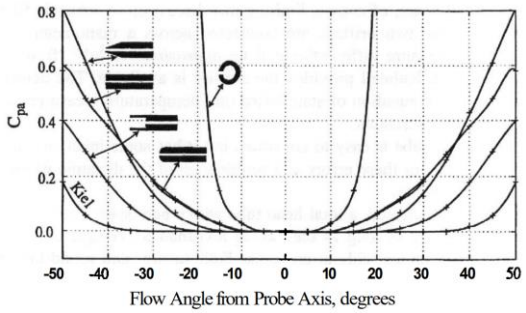

Figure 56. Variation of measured stagnation pressure with yaw for selected probe geometries

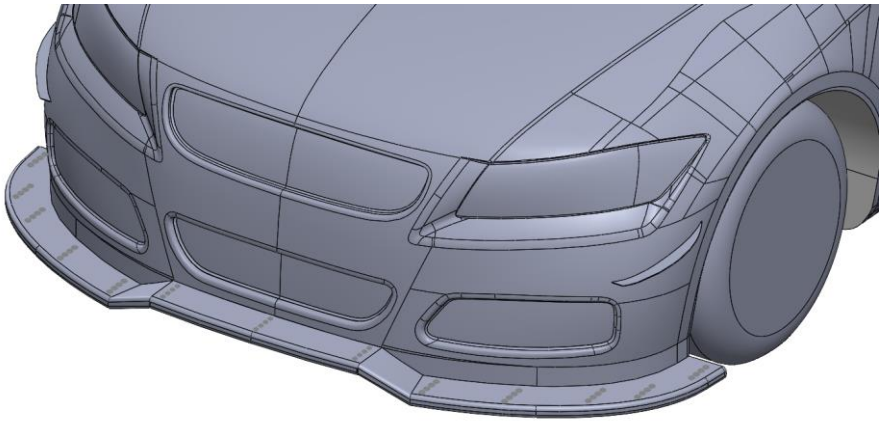

Figure 57. Front Splitter Upper pressure tapings

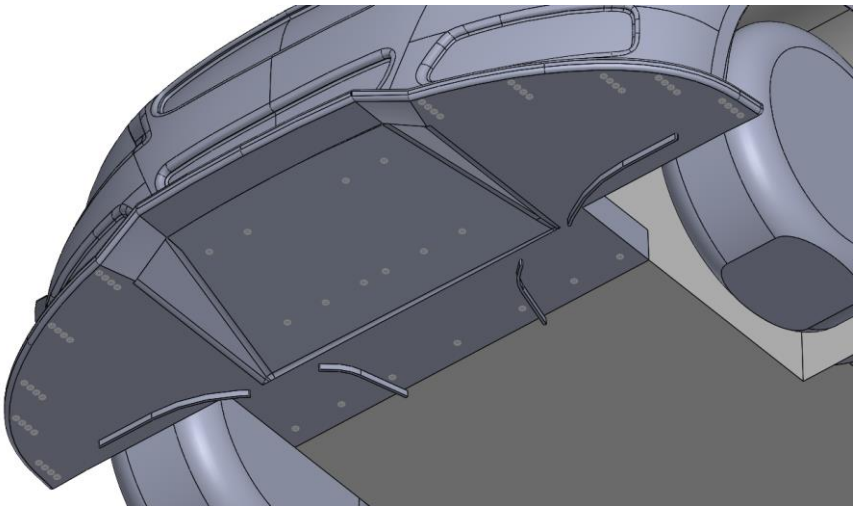

Figure 58. Front Splitter Lower pressure tapings

TESTING PROTOCOL

Table 5. Wind tunnel testing protocol

Wind Tunnel testing protocol	Inlet nozzle speed (km/h)	5-belt floor speed (km/h)	Yaw angle (Degrees)	Measurement devices
Run 1	180	0	0	Pitot tubes in free stream and in front of splitter, pressure taps on splitter surface.
Run 2	180	180	0	Pitot tubes in free stream and in front of splitter, pressure taps on splitter surface, Flowvis on splitter and underbody surface.
Run 2	180	180	0	Pitot tubes in free stream and in front of splitter, pressure taps on splitter surface, Flowvis on splitter and underbody surface.
Run 3	180	180	5	Pitot tubes in free stream and in front of splitter, pressure taps on splitter surface, Flowvis on splitter and underbody surface.
Run 4	180	180	10	Pitot tubes in free stream and in front of splitter, pressure taps on splitter surface, Flowvis on splitter and underbody surface.
Run 5	180	180	15	Pitot tubes in free stream and in front of splitter, pressure taps on splitter surface, Flowvis on splitter and underbody surface.
Run 6	300	0	0	Pitot tubes in free stream and in front of splitter, pressure taps on splitter surface, Flowvis on splitter and underbody surface.

Run 1:	Validate base vehicle performance
Run 2:	Validate aero-package performance
Run 3:	Validate behaviour at 5 degrees of yaw angle
Run 4:	Validate behaviour at 10 degrees of yaw angle
Run 5:	Validate behaviour at 15 degrees of yaw angle
Run 6:	Validate behaviour at LMGT3 top speed

CONCLUSION

In conclusion, this project successfully created and validated a DrivAer vehicle model to be used for the creation of an aerodynamic package. Said aerodynamic package was also developed successfully, with CAD files being created and CFD testing analysed, the aerodynamic package was successful in improving the overall characteristics of the vehicle, improving flow separation and increasing downforce, all while achieving the requirement of a Cd.A lower than 1.02, achieving a Cd.A of 0.79488.

This project underlines the importance of component's performance validation before implementing them into real-world testing, as it can alleviate costs and make design problems visible even before the components are produced. This project's learnings can be applied not only to the DrivAer model, but to the development of any motorsports related vehicle, proving its foundation values in fluid and vehicle dynamics understanding.

GROUP AND PERSONAL REFLECTION

As the responsible for the frontal area of the project, I should have provided my team with more iterations for the front splitter, as I was too focused on fixing the problems that arouse with the current iteration. As the group participated in weekly meetings, we had a good quality of communication, as we were aware of what everyone in the team was doing along the development of the project. I learned valuable skills for my future engineering career, as I finished the project with an overall boost to my skills, as I learned how to use Star CCM+ proficiently and understand different values.

On my overall contribution to the project, I believe that I accomplished the tasks expected from me, completing a baseline CAD model and CFD simulations, producing the required aero-package frontal area components and testing them in CFD simulations for different ride heights and yaw angles, however, I also believe that I slowed down my team's progress, as I had trouble while meshing the frontal area body-parts for CFD simulation and became to fixated on fixing that issue.

As for the group, I believe it was not a functional group, as I had to perform more tasks than I should have to complete the scope of the project, as my group did not work together most of the time, and I ended up being responsible for producing the baseline, aero-package and yaw angle CAD files and CFD simulations present on this report all by myself, without contributions by my teammates, essentially being a one-man team. I believe the scope of the project created an environment where everyone was too focused on finishing their own parts and reports, without thinking about the group aspect of the project.

In summary, I feel that this project has taught me a lot, as I have improved my general knowledge of aerodynamics in a way that can be transferred to more general fluid dynamics, as well as improved my knowledge of the effects that different bodywork can have on the behaviour of the vehicle. My knowledge of Star CCM+ has improved greatly, and I have also noticed improvements in my ability to create CAD files.

I feel that this project has honed my overall engineering skills, and the lessons learned, both theoretical and practical, will be of great value in most of my future projects.

REFERENCES

Versteeg, H.K. and Malalasekera, W., 2007. An Introduction to Computational Fluid Dynamics: The Finite Volume Method. 2nd ed. Harlow: Pearson Education

Barlow, J.B., Rae, W.H. Jr., and Pope, A., 1999. Low-Speed Wind Tunnel Testing. 3rd ed. New York: Wiley.

Qin, P., Ricci, A. and Blocken, B., 2024. CFD simulation of aerodynamic forces on the DrivAer car model: Impact of computational parameters, ScienceDirect. Available at: https://doi.org/10.1016/j.jweia.2024.105711

Soares, R. and Souza, L.F., 2015. Influence of CFD setup and brief analysis of flow over a 3D realistic car model, SAE Technical Paper. Available at: https://doi.org/10.4271/2015-36-0513

Mokhtar, W. A. and Lane, J., 2008. Racecar Front Wing Aerodynamics. SAE Technical Paper 2008-01-2988. Available at: https://doi-org.oxfordbrookes.idm.oclc.org/10.4271/2008-01-2988

Xiao, Q., Khalighi, B., and Tornabene, G., 2014. Aerodynamic Optimization of Race Car Diffuser Geometry Using CFD. SAE Technical Paper 2014-01-0613. Available at: https://doi-org.oxfordbrookes.idm.oclc.org/10.4271/2014-01-0613

Ko, J., and Johnson, A., 2015. Aerodynamic Balance Optimization of a Race Car Using CFD and Wind Tunnel Testing. SAE Technical Paper 2015-01-1538. Available at: https://doi.org/10.4271/2015-01-1538

Bai, K., and He, L., 2018. Aerodynamic and Handling Improvement of a Race Car with Integrated Front and Rear Wings. SAE Technical Paper 2018-01-0725. Available at: https://doi.org/10.4271/2018-01-0725

Bhattacharjee, S., Arora, B. and Kashyap, V., 2019. Optimization of Race Car Front Splitter Placement Using CFD. SAE Technical Paper 2019-01-5097. Available at: https://doi-org.oxfordbrookes.idm.oclc.org/10.4271/2019-01-5097

Chiang, I. Y. and Wan, T., 2021. On the drag reduction optimization of the drivaer fastback model car with digital side mirror. SAE International Journal of Passenger Cars - Mechanical Systems, 06-14-01-0005. Available at: https://doi.org/10.4271/06-14-01-0005

Nakata, A., Okamoto, S., Morikawa, Y., and Nakashima, T., 2023. Effects of Detailed Tire Geometry and Wheel Rotation on the Aerodynamic Performance of Deflectors. International Journal of Automotive Engineering, 14(4), pp.84-91. Available at: https://doi.org/10.20485/jsaeijae.14.4_84

Wieser, D., et al., 2014. Experimental Comparison of the Aerodynamic Behavior of Fastback and Notchback DrivAer Models. SAE International Journal of Passenger Cars - Mechanical Systems, 7(2), pp.682-691. Available at: https://doi.org/10.4271/2014-01-0613

Nagle, P., et al., 2023. The Ford Rolling Road Wind Tunnel Facility. SAE Technical Paper 2023-01-0654. Available at: https://doi.org/10.4271/2023-01-0654

Technische Universität München, n.d. DrivAer Model – Automotive Research Group. Available at: https://www.epc.ed.tum.de/en/aer/research-groups/automotive/drivaer/

SimScale Community, n.d. How to Calculate the Aerodynamic Balance of a Racecar. Available at: https://www.simsxcale.com/forum/t/how-to-calculate-the-aerodynamic-balance-of-a-racecar/96845

DEFINITIONS, ACRONYMS, ABBREVIATIONS

RANS: Reynolds-Averaged Navier-Stokes

RRWT: Ford Rolling Road Wind Tunnel

MGP: Moving Ground Plane

PIV: Particle Image Velocimetry

PSP: Pressure-Sensitive Paint

APPENDIX

OPTIMIZED MESH CONFIGURATION

Table 6. Star CCM+ Optimized mesh settings

Meshers					
Mesher	Setting	Value			
Surface Remesher	Meshing method	Enhanced Quality Triangle			
	Minimum Face Quality	0.05			
Automatic Surface Repair					
Polyhedral Mesher					
Prism Later Mesher	Distribution mode	Wall thickness			
	Gap Fill Percentage	49			
	Layer Reduction Percentage	40			
Default Controls					
Setting	Sub-setting	Value		Units	
Base Size		0.3		m	
Minimum Surface Size	Absolute Size	0.012		m	
Surface Curvature	# Pts/circle	100			
Surface Proximity	# Points in gap	20			
Surface Grow Rate		Slow			
Auto-Repair Minimum...		0.01			
Number of Prism Layers		12			
Prism Layers Near Wall		0.014		mm	
Prism Layer Total Thickness	Absolute Size	30		mm	
Volume Growth Rate		1.1			
Prism Layer Stretching		1.2			
Volume Growth Rate	Default Growth Rate	Custom			
		Nº of Growth layers	6		
	Surface Growth Rate	Very Slow			
Maximum Cell Size	Percentage of Base	1000			
Custom Controls					
Control	Applied on	Controls	Controls Values	Value	Units
Surface Control	Vehicle, wheels and aeropackage	Target Surface Size	Absolute Size	25	mm
		Minimum Surface Size	Relative to base	2	
		Surface Growth Rate	User Specified	1.05	
		Wake Refinement	Size Type	Relative to base	
			Distance	8	m
			Spread Angle	30	deg
			Isotropic Size	Percentage of Base	25
			Wake Refinement	Growth Rate	1.3
Surface Control	Domain	Target Surface Size	Relative to base	100	
Surface Control	Domain Floor	Target Surface Size	Absolute	0.22	m
		Surface Growth Rate		Slow	

OPTIMIZED MESH CONTINUA PHYSICS CONFIGURATION

Table 7. Star CCM+ Continua physics settings

Models	Initial conditions		
All Y+ Wall Treatment	Setting	Values	Units
Constant Density	Pressure	0	Pa
Coupled Flow	Turbulence Intensity	0.03	Constant
Gas	Turbulence Specification	Intensity+Viscosity Ratio	
Gradients	Turbulent Velocity Scale	5	m/s
K-Omega Turbulence	Turbulent Viscosity Ratio	10	
Keynolds-Averaged Navier-Stokes	Velocity	50	m/s
Solution Interpolation			
SST K-Omega			
Steady			
Three Dimensional			
Turbulent			
Wall Distance			

SPLITTER CAD DRAWING

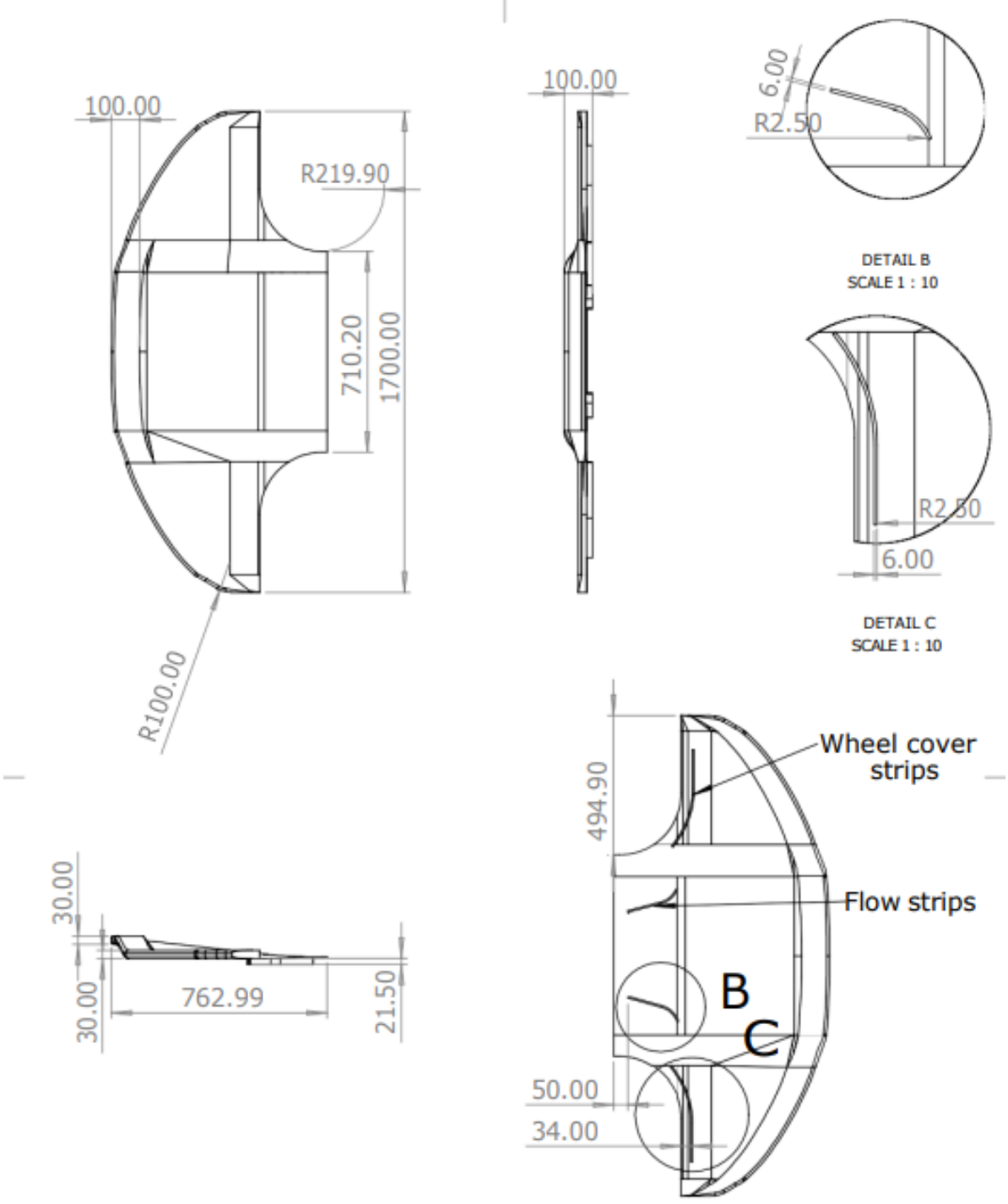

UNLESS OTHERWISE SPECIFIED: DIMENSIONS ARE IN MILLIMETERS SURFACE FINISH: TOLERANCES: LINEAR: ANGULAR:		FINISH:		DEBURR AND BREAK SHARP EDGES		DO NOT SCALE DRAWING	REVISION
	NAME	SIGNATURE	DATE			TITLE:	
DRAWN			20/12/2024			Front Splitter Gr-54	
CHK'D			20/12/2024				
APP'D			20/12/2024				
MFG			20/12/2024				
Q.A			20/12/2024	MATERIAL: Aluminium		DWG NO.	A4
				WEIGHT:		SCALE: 1:20	SHEET 1 OF 1